

# Consistent simulations of multiple proxy responses to an abrupt climate change event

A. N. LeGrande<sup>\*†</sup>, G. A. Schmidt<sup>\*</sup>, D. T. Shindell<sup>\*</sup>, C. V. Field<sup>\*</sup>, R. L. Miller<sup>\*</sup>, D. M. Koch<sup>\*</sup>, G. Faluvegi<sup>\*</sup>, and G. Hoffmann<sup>\*</sup>

<sup>\*</sup>National Aeronautics and Space Administration Goddard Institute for Space Studies and Center for Climate Systems Research, Columbia University, New York, NY 10025; and <sup>†</sup>Laboratoire des Sciences du Climat et l'Environnement/Commissariat à l'Energie Atomique, Orme des Merisiers, 91191 Gif sur Yvette, France

Communicated by James E. Hansen, Goddard Institute for Space Studies, New York, NY, November 22, 2005 (received for review September 22, 2005)

Isotope, aerosol, and methane records document an abrupt cooling event across the Northern Hemisphere at 8.2 kiloyears before present (kyr), while separate geologic lines of evidence document the catastrophic drainage of the glacial Lakes Agassiz and Ojibway into the Hudson Bay at approximately the same time. This melt water pulse may have been the catalyst for a decrease in North Atlantic Deep Water formation and subsequent cooling around the Northern Hemisphere. However, lack of direct evidence for ocean cooling has lead to speculation that this abrupt event was purely local to Greenland and called into question this proposed mechanism. We simulate the response to this melt water pulse using a coupled general circulation model that explicitly tracks water isotopes and with atmosphere-only experiments that calculate changes in atmospheric aerosol deposition (specifically <sup>10</sup>Be and dust) and wetland methane emissions. The simulations produce a short period of significantly diminished North Atlantic Deep Water and are able to quantitatively match paleoclimate observations, including the lack of isotopic signal in the North Atlantic. This direct comparison with multiple proxy records provides compelling evidence that changes in ocean circulation played a major role in this abrupt climate change event.

North Atlantic Deep Water | paleoclimate

The last major abrupt climate change occurred at  $\approx 8.2$  kiloyears before present (kyr) and is recorded in multiple proxy records across the Northern Hemisphere (1). Contemporaneously, glacial Lakes Agassiz and Ojibway catastrophically drained into the Hudson Bay (2, 3), possibly delivering enough freshwater into the North Atlantic to affect the ocean circulation (4, 5). Modeling studies consistently indicate that freshwater pulses into the North Atlantic slow down North Atlantic Deep Water (NADW) formation (6, 7), leading to regional cooling around the North Atlantic Basin and southward shifts in precipitation bands. These results have been interpreted as being consistent with paleoclimate evidence for regional climate changes at 8.2 kyr (1, 8), even though direct evidence for the event in the North Atlantic Ocean is sparse. One problem is that longer-term variability, possibly linked to solar activity, is coincident with an abrupt signal at 8.2 kyr (9), making clear association of proxy records to a melt water pulse (MWP) event difficult.

Proxy records of  $\delta^{18}\text{O}_{\text{precip}}$  (where  $\delta$  indicates a comparison of the concentration of the tracer in the subscripted sample to that in standard mean ocean water), including ice cores, lake sediment cores, and speleothems (cave deposits), are used to infer local past temperature conditions as well as past relative precipitation because there is a strong observed correlation between increased rainfall and/or decreased temperature and depleted  $\delta^{18}\text{O}_{\text{precip}}$ . The 8.2-kyr event is clearly expressed in Greenland ice core records as a 2‰ depletion; this change has been interpreted to imply a decrease in surface air temperature (SAT) of up to 6°C (1). In Ammersee, Germany, this event is expressed as a 1‰ depletion in the interpreted isotopic composition of lake water; this change implies a 1.7°C temperature decrease (5). In

the East Norwegian Sea,  $\delta^{18}\text{O}_{\text{calcite}}$ , a proxy for ocean temperature, records a 0.7‰ enrichment [analogous to a decrease in temperature of 3–4°C (10), assuming little change in the isotopic composition of seawater].

However, other factors including isotopic composition of the original evaporate and distance from source region also impact  $\delta^{18}\text{O}_{\text{precip}}$ . Thus, patterns of  $\delta^{18}\text{O}_{\text{precip}}$  change are more complex than temperature or precipitation patterns alone, highlighting the importance of including isotopic tracers to assist in accurate proxy interpretation.

Additional independent constraints on hemispheric climate change can be derived from the ice core records of methane and aerosols. Changes in ice core methane concentration reflect larger-scale changes in methane sources (11), which during preindustrial times were dominated ( $\approx 75\%$ ) by wetlands (12). Greenland Ice Sheet Project Two (GISP2) and Greenland Ice Core Project (GRIP) ice cores show that methane concentration sharply decreases by  $\approx 10\text{--}15\%$  [ $\approx 75$  parts per billion by volume (ppbv)] (4). Ice cores contain a record of aerosol concentrations such as dust and <sup>10</sup>Be (which attaches to sulfate aerosols) that reflect regional climate conditions. The concentration of the cosmogenic isotope <sup>10</sup>Be increases by  $\approx 40\%$  in the GRIP ice core (13), whereas dust concentration increases by up to 60% (4). Aerosol concentration increases indicate regional circulation and hydrologic changes.

A fundamental issue is that proxy records are necessarily indirect measures of climate change that often reflect changes in multiple aspects of climate. Thus, the incorporation of relevant tracers in general circulation models (GCMs) is required for direct model–data comparisons. Previous studies of MWP impacts have used water isotope tracers (14), but this study fully implements them in a coupled GCM. Moreover, we incorporate three additional tracers to use a truly multiproxy approach. Our goal is to assess whether a MWP into the Hudson Bay could have produced the observed abrupt climate change 8.2 kyr ago.

## Results

In several coupled GCM simulations, we add isotopically depleted freshwater into the Hudson Bay. We vary the rate and volume of these MWPs, as well as ocean initial conditions, characterized by strong and weak NADW production (see *Methods* for full description). We focus on the simulations that apply 2.5 and 5 Sverdrup (Sv) yr (1 Sv =  $10^6$  m<sup>3</sup>/s; 1 Sv yr =  $0.315 \times 10^{14}$  m<sup>3</sup>) pulses over 0.5 or 1 yr because this range is the most consistent with recent hydrologic model estimates for the volume and duration of this event (2).

All simulations show a significant decrease in NADW production; as in earlier studies (6), the exact structure of the global

Conflict of interest statement: No conflicts declared.

Abbreviations: GCM, general circulation model; kyr, kiloyears before present; MWP, melt water pulse; NADW, North Atlantic Deep Water; SAT, surface air temperature; SST, sea surface temperature.

<sup>†</sup>To whom correspondence should be addressed. E-mail: legrande@giss.nasa.gov.

© 2006 by The National Academy of Sciences of the USA

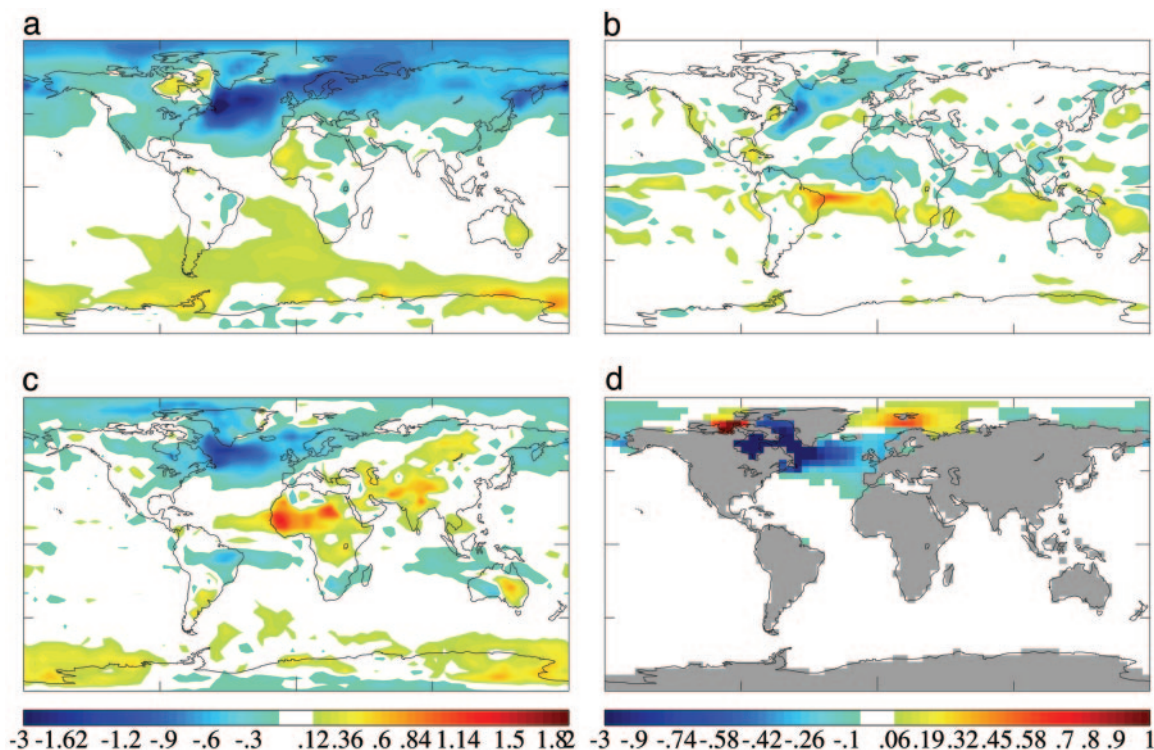


**Fig. 1.** The effective climate response in five simulations (with 2.5 and 5 Sv yr of melt water introduced to the Hudson Bay) given a 40% reduction (the ensemble average) in overturning circulation. Only grid boxes with a high (0.5) goodness of fit appear. (a) SAT changes ( $^{\circ}\text{C}$ ). (b) Precipitation changes (mm/day). (c)  $\delta^{18}\text{O}_{\text{precip}}$  anomalies. Increased rainfall and decreased temperature cause  $\delta^{18}\text{O}_{\text{precip}}$  depletions making the structure of  $\delta^{18}\text{O}_{\text{precip}}$  changes (‰) more complicated than either field. (d) Changes in  $\delta^{18}\text{O}_{\text{seawater}}$  (‰) show depletion in the North Atlantic due to the depleted melt water and reduced transport of enriched seawater from the subtropics. At  $>60^{\circ}\text{N}$ , increased sea ice (or reduced melting) leads to surface water enrichments.

climate responses across these simulations is stochastic. The greatest volume of freshwater input neither creates the largest amplitude nor the longest duration of diminished NADW production. The mean percentage decrease in decadal-mean NADW formation is 40% ( $1\sigma = 11\%$ ) with the maximum slowdown occurring 8–16 yr after the MWP. The overturning initially recovers in all of the simulations after 20–30 years. However, the runs with weaker initial NADW production undergo secondary (and tertiary) slowdowns and recoveries in overturning strength on multidecadal timescales. In the weak NADW cases, full recovery takes almost 200 yr, whereas it requires much less than 100 yr for recovery in the strong NADW case.

Decreased NADW formation leads to decreased ocean heat transport. Greater atmospheric heat transport compensates in part for this deficit, but overall northward heat transport in the North Atlantic decreases by  $\approx 0.3$  PW over the ensemble.

Changes in NADW production are closely correlated with alterations in the upper-ocean temperature structure of the Atlantic and subsequent related climate changes. As a consequence of the cooler ocean temperatures, higher pressure as well as general drying occurs across the North Atlantic Basin and Mediterranean. Storm tracks become more zonal in the Atlantic, resulting in less rainfall poleward of the North Atlantic Drift. Additionally, cooling in the north shifts the Inter-Tropical Convergence Zone southward in all ocean basins consistent with interpretations of ocean sediment core records offshore of Venezuela (15) and corroborating previous studies (16).

Because timescales and magnitude of response of the modeled climate vary across all simulations, we use the decadal-mean NADW (percent) anomaly as a simple index to extract a consistent global response from the model, reducing the effects

of the timing, duration, and “weather” associated with individual realizations. For each experiment we use this NADW anomaly index as an independent variable against which we regress the sea surface temperature (SST), SAT, sea ice, sea-level pressure, precipitation, and isotope ( $\delta^{18}\text{O}_{\text{precip}}$ ,  $\delta^{18}\text{O}_{\text{seawater}}$ ,  $\delta^{18}\text{O}_{\text{calcite}}$ ) anomalies at each grid box. This linear regression is appropriate here despite potential nonlinear feedbacks because (i) the size of the MWP forcing is relatively small and (ii) it serves to demonstrate more clearly the first-order response. This regression then is scaled to the  $-40\%$  mean NADW response across all of the five-member ensemble runs, and it defines the mean decadal response of the model to the MWP even above a background of decadal scale variability and different time scales and response magnitudes of the various ensemble members (Fig. 1).

Comparisons of the ensemble mean response to the results seen in individual runs suggest this method is a reasonable one for extracting the consistent model response to the MWP forcing, with the additional benefit that the illustrated changes are robust over the ensemble members.

The greatest temperature decreases occur across the North Atlantic region with the largest anomalies in the northern North Atlantic. Some cooling ( $\approx 1^{\circ}\text{C}$ ) extends across the Northern Hemisphere, with significant terrestrial cooling over Greenland, Europe, and parts of North America. Southern Hemisphere temperatures remain largely unchanged, with the exception of mild warming over parts of the South Atlantic and Southern Ocean (Fig. 1a). The contrast in response between the Northern and Southern hemispheres is an expression of the bipolar seesaw (17).

**Water Isotopes.** Comparisons of the simulation to Greenland ice core proxy records are crucial; however, the modeled accumulation at the Summit grid box (accumulation 0.14 mm/day; mean annual

**Table 1. Comparisons of isotopic proxy records with coupled model isotope and temperature fields at relevant grid boxes**

Location	Data $\delta^{18}\text{O}$ , ‰	Ensemble excursion				Temporal slope T & $\delta^{18}\text{O}$ , ‰/°C
		$\delta^{18}\text{O}$ (‰)		Temperature, °C		
		Mean	Range	Mean	Range	
Summit, Greenland	−2	−1.0	−1.2:−0.8	−1.4	−1.9:−1.1	0.25 ( $r = 0.37$ )
Summit average, Greenland		−0.9	−1.0:−0.7	−1.3	−1.6:−0.9	0.30 ( $r = 0.53$ )
British Isles	*	−0.9	−1.3:−0.7	−1.1	−1.3:−0.8	0.72 ( $r = 0.43$ )
Ammersee, Germany	−1	−0.6	−0.9:−0.2	−0.4	−0.2:−0.5	0.40 ( $r = 0.77$ )
East Norwegian Sea	0.7	0.3	0.1:0.6	−2.1	−3.3:−1.4	−0.15 ( $r = 0.75$ )

All comparisons are at decadal time scales for the most appropriate comparison with the proxy records. For Greenland and Ammersee, we compare  $\delta^{18}\text{O}_{\text{precip}}$  to the  $\delta^{18}\text{O}_{\text{ice}}$  (4, 32) and  $\delta^{18}\text{O}_{\text{precip}}$  (5). We report the value of  $\delta^{18}\text{O}_{\text{precip}}$  for the British Isles. In the East Norwegian Sea, we compare the model and data surface ocean  $\delta^{18}\text{O}_{\text{calcite}}$ . The table shows the largest magnitude excursion (negative for the atmospheric proxies and temperature, positive for the ocean proxies) and the range over all the ensemble members. The mean relationship and correlation ( $r$ ) between the decadal mean anomaly proxies and local temperature over all simulations are also shown. For calcite-based proxies, there is a temperature-dependent fractionation (approximately  $-0.2\text{‰}/^\circ\text{C}$ ), which we apply for the ocean proxy, but not for the terrestrial records because the relevant temperature is more difficult to diagnose from the model. The inferred decadal temperature change at Summit ranges from approximately  $-3.6$  to  $-6^\circ\text{C}$  (4, 5).

temperature  $-30^\circ\text{C}$ ; mean  $\delta^{18}\text{O}_{\text{precip}} -34\text{‰}$ ) is sufficiently different from observed (0.55 mm/day;  $-31^\circ\text{C}$ ;  $-34\text{‰}$ ) to cause concern. Thus, we report results from both the Summit grid box and a wider average (incorporating the grid boxes immediately to the south and east of Summit) that better correspond to observed (0.54 mm/day;  $-28^\circ\text{C}$ ;  $-34\text{‰}$ ) (Table 1).

The local relationship between SAT and  $\delta^{18}\text{O}_{\text{precip}}$  is crucial to inferring temperature from a proxy record of  $\delta^{18}\text{O}_{\text{precip}}$ . However, this relationship could be variable through time, particularly in periods of abrupt climate change. A further complication in a MWP event is the introduction of isotopically depleted water that can change the initial isotopic concentration of the evaporate (toward more depleted values, implying cooler temperatures). The modeled SAT– $\delta^{18}\text{O}_{\text{precip}}$  relationship (Fig. 2a) is consistent with observational and paleoclimate evidence (Table 1). In particular, the relationship at Summit, Greenland, agrees well with paleoclimate evidence [modeled values  $0.25\text{--}0.3^\circ\text{C}$  compared with an inferred temporal gradient of  $\approx 0.33\text{--}0.38^\circ\text{C}$  (18, 19)]; however, the correlation coefficient is small,  $r = 0.3$  (Table 1).

Despite decreases in rainfall (which typically enriches the signal),  $\delta^{18}\text{O}_{\text{precip}}$  depletion associated with cooler temperatures occurs across the North Atlantic region (Fig. 1c). The southward shift of the Inter-Tropical Convergence Zone yields bands of enriched  $\delta^{18}\text{O}_{\text{precip}}$  in the northern subtropics and depleted  $\delta^{18}\text{O}_{\text{precip}}$  to the south. Some speleothem evidence from Costa Rica has suggested such a shift (20), but our modeled anomalies in  $\delta^{18}\text{O}_{\text{precip}}$  do not extend to this area.

The strongest cooling and depletions in  $\delta^{18}\text{O}_{\text{precip}}$  occur during boreal winter (with roughly twice the change observed in the annual average) (cf. ref. 21). A reduction in winter precipitation decreases the weighting of annual  $\delta^{18}\text{O}_{\text{precip}}$  changes toward the wetter (summer) months. Fig. 1 illustrates that the patterns of  $\delta^{18}\text{O}_{\text{precip}}$  change are more complex than the temperature or precipitation patterns alone; furthermore, the  $\delta^{18}\text{O}_{\text{precip}}$ –SAT relationship can vary on shorter timescales.

In the ocean, surface  $\delta^{18}\text{O}_{\text{seawater}}$  becomes depleted in the northern North Atlantic because of both the reduced northward transport of enriched tropical surface water and the addition of depleted melt water. At high latitudes, increases in sea ice lead to increases in  $\delta^{18}\text{O}_{\text{seawater}}$  (Fig. 1d).

Cooler ocean temperatures enrich  $\delta^{18}\text{O}_{\text{calcite}}$  (by  $\approx 1\text{‰}$  per  $5^\circ\text{C}$  cooling) and oppose the seawater depletion (in the Atlantic between  $\approx 50^\circ\text{N}$  and Iceland), which causes the rela-

tionship between SST and  $\delta^{18}\text{O}_{\text{calcite}}$  to break down (Fig. 2b). One of the most enigmatic proxy results for the 8.2-kyr event is its apparent absence in much of the North Atlantic. Fig. 3f illustrates the competing effects in  $\delta^{18}\text{O}_{\text{calcite}}$ : for the simula-

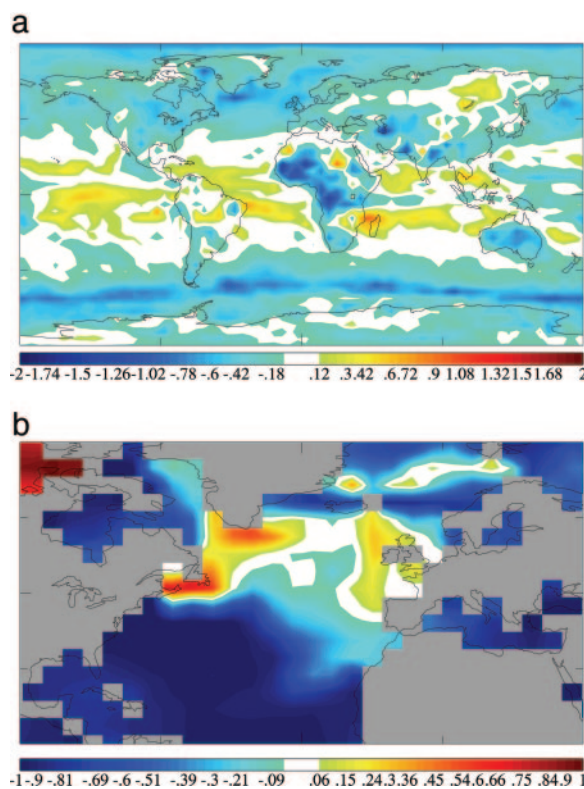


**Fig. 2.** Proxy validation for model simulations indicates the relationship between  $\delta^{18}\text{O}$  and temperature in the atmosphere and ocean. (a) The temporal gradient in SAT vs.  $\delta^{18}\text{O}_{\text{precip}}$  (‰/°C), the relationship crucial for interpreting many atmospheric paleoclimate records, is steepest and most highly correlated at high latitudes and is very shallow or reversed with lower correlation in the subtropics and tropics. (b) The correlation of SST vs.  $\delta^{18}\text{O}_{\text{calcite}}$ , the relationship crucial for interpreting many sediment core paleoclimate records, breaks down in most of the northern North Atlantic, with the exception of areas along the northern Greenland, Iceland, and Norwegian (GIN) Seas.

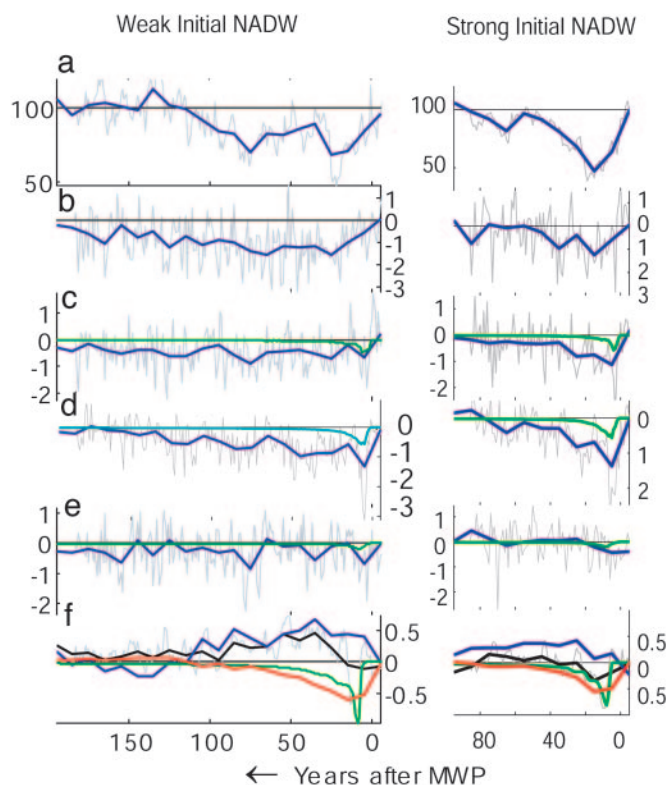


**Fig. 3.** Selected time series for two simulations (weak and strong initial NADW, 5 Sv for 1 yr case) (see Data Sets 1 and 2 for the other individual simulations). Lines represent decadal (blue, red, and black) or annual (gray and green) departures from the 30-yr mean in the relevant control. (a) Percent change in NADW production. (b) Modeled temperature change for three grid boxes near Summit in degrees Celsius. (c–f) Green line is the scaled MWP contribution to the  $\delta^{18}\text{O}$  signal. (c) Modeled  $\delta^{18}\text{O}_{\text{precip}}$  for three grid boxes near Summit (‰). (d) Modeled  $\delta^{18}\text{O}_{\text{precip}}$  for the British Isles (‰). (e) Modeled  $\delta^{18}\text{O}_{\text{precip}}$  for Ammersee, Germany (‰). (f) Modeled ocean changes in the East Norwegian Sea, the change in  $\delta^{18}\text{O}_{\text{calcite}}$  (black), and the separate temperature (blue) and seawater (red) components (‰).

tion with weak initial NADW, initially, the effects of seawater depletion minimize the recorded signal in the calcite, but by yr 30 the temperature signal becomes dominant. However, in the simulation with strong initial NADW, the  $\delta^{18}\text{O}_{\text{seawater}}$  dominates the signal. The difference between the two runs is the difference between the precise grid box (front) where the temperature effect or  $\delta^{18}\text{O}_{\text{seawater}}$  effect on  $\delta^{18}\text{O}_{\text{calcite}}$  becomes more dominant.

For this specific size and length of MWP, these factors dampen or eliminate changes in  $\delta^{18}\text{O}_{\text{calcite}}$ , with the exception of the northern Greenland, Iceland, and Norwegian (GIN) Seas where increases in sea ice (or reduced melting) lead to enriched surface  $\delta^{18}\text{O}_{\text{seawater}}$  and  $\delta^{18}\text{O}_{\text{calcite}}$ . Potentially, the absence of larger depletions in North Atlantic calcite proxy record may put an upper limit on the maximum feasible volume of the event.

Comparisons of the modeled  $\delta^{18}\text{O}$  changes to specific proxy records are shown in Table 1. The modeled responses are the correct order of magnitude and sign, but smaller than those in the corresponding paleoclimate records. In particular, the decadal temperature response at Greenland is significantly smaller than that inferred previously (4), although the isotope values are not as severely underestimated.

The failure to resolve the extremely shallow winter inversion layers over the Greenland ice sheet may lead to underestimates of temperature changes there (18). The lack of sensitivity of

Greenland climate is a general modeling problem seen in other studies (22, 23).

Different timescales and magnitudes of response make compiling transient responses from all individual simulations unclear; thus, we highlight two simulations of 5 Sv yr from each base state (Fig. 3; for other data, see Data Sets 1 and 2, which are published as supporting information on the PNAS web site).

Within the first decade, an initial rain out of evaporated isotopically depleted melt water occurs across the North Atlantic, creating  $\delta^{18}\text{O}_{\text{precip}}$  depletions unrelated to temperature. Fig. 3 c–e illustrates this clear temporary source effect from depleted melt water (green lines) in the  $\delta^{18}\text{O}_{\text{precip}}$  of up to  $-0.8\text{‰}$  at the British Isles,  $-0.5\text{‰}$  in Greenland, and  $-0.2\text{‰}$  in Ammersee. Subsequent cooling episodes and related  $\delta^{18}\text{O}_{\text{precip}}$  depletions are more closely correlated with decreases in SAT and slow-downs in NADW formation. Previous studies suggested that the double spike in  $\delta^{18}\text{O}_{\text{precip}}$  in some records implied two separate MWPs. Although this scenario cannot be ruled out, our results indicate that it is not required because both the rain out of depleted melt water and cycles of weaker overturning (such as in MWP simulations using the weak NADW base case) create multiple spikes of depleted  $\delta^{18}\text{O}$ .

Is the coupled model response to the MWP forcing reasonable? The water isotope results indicate that the average decadal mean change in the ensemble underestimates the signal seen in the proxy records; however, the maximum response is closer. This result may indicate that either the MWP magnitudes applied in the experiments are too small (although experiments with doubled volumes of melt water did not produce significantly different results), that the model is not sufficiently sensitive (e.g., in the NADW response or at the local grid box scale), or that the initial mechanism is incorrect. We therefore examine a suite of other proxies to address these possibilities.

**Other Ice Core Proxy Records.** We force the atmosphere-only version of Goddard Institute for Space Studies MODELE ([www.giss.nasa.gov/tools/modelE](http://www.giss.nasa.gov/tools/modelE)) with SST and sea ice conditions extracted from the coupled model and assess the climate impacts on cosmogenic isotope deposition ( $^{10}\text{Be}$ ) (24), dust (25), and wetland methane emissions (26). Two sets of boundary conditions were produced: one corresponding to the mean maximum decadal response (a 40% reduction in NADW production) and the other corresponding to the maximum (60%) decrease. All results shown are 10-yr means except for the methane simulations, for which only 5 yr are used (Fig. 4).

Both the aerosol tracers ( $^{10}\text{Be}$  and dust) are advected, gravitationally settled, turbulently deposited, and affected by the hydrological cycle through dissolution and impaction (25). The production function for  $^{10}\text{Be}$  is appropriate for mean solar activity over the last 50 yr and the present-day magnetic field (27). Dust sources are parameterized based on a subgrid-scale wind distribution and present-day distribution of “preferred” sources using a topographic criterion (25). Aerosol ice core concentration is calculated by dividing the total dry and wet deposited flux by snow accumulation. The results we report include an average of several grid boxes around Summit making the inferred anomalies more robust. The model response for all aerosol species shows concentration increases due to increased deposition and reductions in snow accumulation that are close to the observed ice core changes (Fig. 4). The simulated concentration of dust increases by 11% (–40% NADW case) and 21% (–60% NADW case), and both scenarios indicate an increase in dust load over Greenland.

The modeled concentration of  $^{10}\text{Be}$  increases by 24% (–40% NADW case) and 35% (–60% NADW case), reflecting an increase in both wet and dry deposition. These changes in  $^{10}\text{Be}$  are purely climatic because no solar-related change in production was applied. The concentration of  $^{10}\text{Be}$  is widely considered to be a proxy for

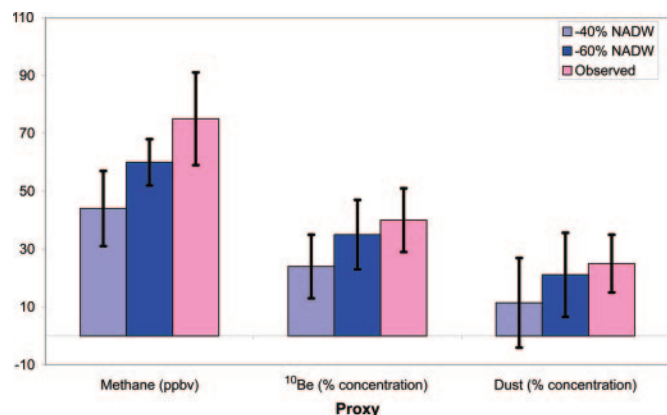


**Fig. 4.** Comparison of Greenland ice core data with multiproxy results from the atmosphere-only GCM given SST and sea ice changes from the coupled model scaled for 40% and 60% reductions in NADW. (*Left*) Global methane concentration decrease. (*Center*) Summit average  $^{10}\text{Be}$  percent change in concentration. (*Right*) Summit average dust percent change in concentration. The observed changes in dust are derived by using the 50-yr mean concentrations immediately before the event (8,250 kyr in the Greenland Ice Sheet Project Two core) compared with the 50-yr mean around the peak (33). Larger changes (up to 60%) for the dust can be inferred by using the minimum concentration 100 yr earlier and a shorter averaging period (4). Sixty-year means are used for the  $^{10}\text{Be}$  because of the coarser resolution of Greenland Ice Core Project core data (13). Error bars ( $1\sigma$ ) are for the measurement and sampling uncertainty in the observations and the sampling uncertainty in the models based on the interannual variability.

solar irradiance changes because it is produced by interactions between atmospheric oxygen and nitrogen and cosmic rays, which are related to changes in the sun's magnetic field. Thus, the modeled climatic impacts on  $^{10}\text{Be}$  concentration complicate estimates of potentially coincident solar changes (24).

The principle cause of both aerosol changes is a reduction in precipitation around the Northern North Atlantic and a subsequent increase in the residence time and aerosol concentrations in this region. Because most Greenland dust sources are Asian, neither increases in the Saharan dust source nor the uncertainty related to dust sources at  $\approx 8$  kyr, is likely to impact the modeled sensitivity.

Methane emissions are calculated online by using local regression models for temperature and precipitation combined with an assessment of the viability of wetlands using soil moisture characteristics and local climate (26). The subsequent concentration calculations are for global mean abundance; any decrease in the hemispheric gradient would increase the change seen at Greenland (11).

The wetland emissions model is sensitive to changes in temperature and precipitation that modulate methane production and the spatial extent of viable wetland areas (26). Decreases in temperature and precipitation over North America and Europe cause a decrease in wetlands methane emission of 8% and 11%. In both cases, reductions from boreal areas (poleward of 30°N) are about twice as large those from tropical areas (0–30°N). Once the influence of methane on its own lifetime is accounted for, these changes in emissions imply 9% and 12% decreases in global methane atmospheric abundance (equivalent to 44 and 60 ppbv given a starting concentration of 650 ppbv), consistent with but slightly less than the  $75 \pm 8$  ppbv decrease recorded in Greenland ice cores (28, 8). Given this magnitude of the methane changes, a less widespread event

$\approx 8.2$  kyr ago would be difficult to reconcile with the methane data.

## Conclusions and Discussion

Our simulations of the 8.2-kyr event with very distinct tracers provide a set of tools to understand consistent model responses to this freshwater forcing. For all tracers, the changes are consistent with observations, particularly in the 60% NADW decrease case. Given an average NADW reduction of 40%, the water isotope excursions are of the correct magnitude but underestimate observed changes. Other independent proxies indicate that reductions in NADW production ranging from 40% to 60% produce similar magnitude excursions in the model as those observed ice core changes. Because melt water has highly depleted  $\delta^{18}\text{O}_{\text{seawater}}$ , simulations with larger ( $2\times$ ) volume create a larger  $\delta^{18}\text{O}_{\text{seawater}}$  depletion across the North Atlantic, which are large enough to have been recorded in  $\delta^{18}\text{O}_{\text{calcite}}$  ocean sediment core records. The absence of such proxy records of  $\delta^{18}\text{O}_{\text{calcite}}$  depletion indicates that a larger MWP forcing for the 8.2-kyr event may not be appropriate. Although uncertainties exist in the model ocean response and in the simulation of individual proxies, the collective response is in qualitative agreement with observations.

These results provide compelling evidence that significant reductions in NADW production by about half are consistent with multiple paleoclimate proxies at 8.2 kyr. Uncertainties in the response of NADW to climate forcing are a key issue in the projection of future climate change. A coupled model's ability to produce a reasonable response to forcing appropriate to the 8.2-kyr event should improve our confidence in the projections of future anthropogenic changes.

## Methods

**Coupled Model and Water Isotopes.** We used a fully coupled atmosphere/ocean GCM (Goddard Institute for Space Studies MODELE) that is also being used for the Intergovernmental Panel on Climate Change AR4 (29). Water isotopes are included in the atmosphere (30), sea ice, and ocean (31) and were tracked through all stages of the hydrologic cycle. The ocean model is non-Boussinesq, mass conserving, and has a full free surface. Freshwater is added in a “natural” way (increasing the free surface and reducing salinity purely through dilution). No equivalent salt fluxes or flux adjustments were used. All boundary conditions and atmospheric composition are appropriate to the preindustrial (circa 1880).

**Event Simulation.** In 12 coupled GCM simulations, we introduced fresh, isotopically depleted water ( $0^{\circ}\text{C}$ ,  $-30\text{‰}$   $\delta^{18}\text{O}_{\text{seawater}}$ ) into the Hudson Bay (adding to the total volume of water in the climate system). Additionally, we added a passive tracer to the melt water to track its movement through the simulation. The results discussed here use a range of volumes from 2.5 to 5 Sv yr, applied from 0.5 to 1 yr. Further experiments with volumes from 1.25 to 10 Sv and applied from 0.25 to 2 yr are qualitatively similar. The range of 2.5 Sv yr ( $\approx 0.788 \times 10^{14} \text{ m}^3$  or  $\approx 23 \text{ cm}$  rise of sea level) to 5 Sv yr ( $\approx 1.576 \times 10^{14} \text{ m}^3$ , 45 cm rise in sea level) is the most consistent with recent hydrologic model estimates for the volume and duration of the 8.2-kyr drainage of glacial Lakes Agassiz and Ojibway (2).

Initial conditions were taken from quasi-stable points in a multicentury control simulation. In half the scenarios, the initial conditions were taken from yr 600 in the control, which had a strong, stable overturning circulation ( $22 \pm 1.2$  Sv NADW formation), whereas in the other simulations the initial conditions came from yr 200, which had weaker, more variable overturning ( $12 \pm 1.7$  Sv). NADW formation is defined here as the Atlantic overturning stream function at  $48^\circ\text{N}$  and 900-m depth. The maximum overturning circulation in the Atlantic is greater but more variable and less robust as an indicator of climate change. Specifically, the five ensemble members consist of experiments that apply melt water at

<sup>§</sup>Kobashi, T., Severinghaus, J. P., Brook, E., Grachev, A. & Barnola, J.-M. (2004) *EOS Trans. AGU Fall Meeting. Suppl.*, abstr. PP31A-0905.

